Multicomponent and High-Pressure Effects on Droplet Vaporization

S. K. Aggarwal
Department of Mechanical Engineering,
University of Illinois at Chicago,
Chicago, IL 60607

H. C. Mongia
GE Aircraft Engines,
Cincinnati, OH 45215

This paper deals with the multicomponent nature of gas turbine fuels under high-pressure conditions. The study is motivated by the consideration that the droplet submodels that are currently employed in spray codes for predicting gas turbine combustor flows do not adequately incorporate the multicomponent fuel and high-pressure effects. The quasi-steady multicomponent droplet model has been employed to investigate conditions under which the vaporization behavior of a multicomponent fuel droplet can be represented by a surrogate pure fuel droplet. The physical system considered is that of a multicomponent fuel droplet undergoing quasi-steady vaporization in an environment characterized by its temperature, pressure, and composition. Using different vaporization models, such as infinite-diffusion and diffusion-limit models, the predicted vaporization history and other relevant properties of a bicomponent droplet are compared with those of a surrogate single-component fuel droplet over a range of parameters relevant to gas turbine combustors. Results indicate that for moderate and high-power operation, a suitably selected single-component (50 percent boiling point) fuel can be used to represent the vaporization behavior of a bicomponent fuel, provided one employs the diffusion-limit or effective-diffusivity model. Simulation of the bicomponent fuel by a surrogate fuel becomes increasingly better at higher pressures. In fact, the droplet vaporization behavior at higher pressures is observed to be more sensitive to droplet heating models rather than to liquid fuel composition. This can be attributed to increase in the droplet heatup time and reduction in the volatility differential between the constituent fuels at higher pressures. For ignition, lean blowout and idle operations, characterized by low pressure and temperature ambient, the multicomponent fuel evaporation cannot be simulated by a single-component fuel. The validity of a quasi-steady high-pressure droplet vaporization model has also been examined. The model includes the nonideal gas behavior, liquid-phase solubility of gases, and variable thermo-transport properties including their dependence on pressure. Predictions of the high-pressure droplet model show good agreement with the available experimental data over a wide range of pressures, implying that quasi-steady vaporization model can be used at pressures up to the fuel critical pressure.
[DOI: 10.1115/1.1423640]

Introduction

The design of advanced gas turbine combustors is increasingly relying upon CFD-based methodologies. To this end, significant advances have been made in the computational capabilities for predicting the detailed structure of reacting two-phase flows in gas turbine combustors. However, several critical issues with regards to the physical-numerical modeling of these flows still remain unresolved. One such issue pertains to the realistic representation of the multicomponent nature of gas turbine fuels. The spray codes that are currently employed in the gas turbine industry are based on a single-component droplet vaporization submodel, although it has been recognized that gas turbine fuels are multicomponent with a wide distillation curve. This raises several questions regarding the applicability of these codes. First, the gasification behavior of multicomponent fuel sprays may be qualitatively different from that of corresponding pure fuel sprays. This would imply that a single-component spray model would not be adequate to predict the realistic fuel vapor distribution in a gas turbine combustor. This would clearly have an impact on the predicted ignition, flame stability, combustion characteristics, and pollutant levels. Second, the detailed and/or reduced chemistry models for hydrocarbon fuels ([1,2]) have generally been developed and validated for pure fuels, and their extension to multicomponent gas turbine fuels may not be straightforward. Third, the methodologies to model turbulent-chemistry interactions for single-component fuels would require modifications for jet fuels, especially for predicting soot.

Another issue pertains to the gasification behavior of an isolated fuel droplet. A multicomponent droplet ([3,4]) is known to exhibit a significantly different gasification behavior compared with that of a pure fuel droplet. These differences have been attributed ([3–9]) to transient liquid mass transport in the droplet interior, volatility differential between the constituent fuels, phase equilibrium at the droplet surface, and thermo-transport properties that are functions of mixture composition, temperature, and pressure. In order to address these complex issues for jet fuels in a systematic manner, we have taken a first step, i.e., study the vaporization behavior of a multicomponent fuel droplet and examine if it can be simulated by a surrogate pure fuel droplet.

In this paper, we examine conditions under which the gasification behavior of a multicomponent fuel droplet may be represented by a surrogate single-component fuel droplet. The range of conditions considered corresponds to the operating range of gas turbine combustors. The state-of-the-art vaporization models ([4–9]) are employed for both the multicomponent and single-component fuel droplets. In particular, the two commonly employed liquid-heating models, namely the infinite-diffusion ([7,9]) model and the diffusion-limit model ([7,9]), are used for both the single and multicomponent-fuel droplets. The objective of using

Contributed by the Combustion and Fuels Division of THE AMERICAN SOCIETY OF MECHANICAL ENGINEERS for publication in the ASME JOURNAL OF ENGINEERING FOR GAS TURBINES AND POWER. Manuscript received by the C&F Division, October 2000; final revision, March 2001. Editor: S. R. Gollahalli.

these models is to assess the effect of transient liquid transport, especially that of temperature and concentration distributions within the droplet interior, on the prediction of droplet vaporization rates under conditions relevant to gas turbine combustors. The thermophysical and transport properties of both the gas phase and liquid phase are calculated in a comprehensive manner. It should be noted that numerous previous studies have examined the gasification behavior of multicomponent fuel droplets. However, none of these studies have focused on the issue of simulating the vaporization behavior of a multicomponent fuel droplet by a surrogate single-component droplet under conditions relevant to gas turbine combustors.

Another objective of the present study is to extend the low-pressure quasi-steady droplet vaporization model to high-pressure conditions including the thermodynamic supercritical state of the liquid fuel. This is motivated by several considerations. First, the modern turbo-propulsion gas turbine combustors operate at pressures approaching or exceeding 40 atmospheres. Second, in high-performance military engines, the liquid fuel is being looked at as the primary coolant for on-board heat sources, and may attain a critical state before it is ''atomized.'' Third, the high-pressure gasification phenomena exhibit characteristics that are distinctly different from those in a low-pressure environment. For example, the gas-phase nonidealities and the liquid-phase solubility, which are negligible at low pressures, must be taken into considerations as the ambient pressure approaches the critical state of the liquid fuel. Finally, the liquid-vapor equilibrium at the droplet surface and the latent heat of evaporation are markedly different at low and high-pressure conditions. Consequently, the conventional low-pressure droplet models may not be valid at pressures near and exceeding the fuel critical pressure.

The transcritical droplet gasification phenomena are also relevant to diesel and liquid rocket engines. Consequently, a number of experimental, analytical, and computational studies have been reported in this area. Experimental studies have employed the porous-sphere ([10]) (for droplet combustion), suspended-droplet ([11]), and freely falling droplet ([12]) configurations to examine the supercritical droplet gasification behavior for a variety of liquid fuels. Computational studies ([13–17]) have often considered an isolated, stationary fuel droplet which is suddenly placed in a high-pressure environment. Detailed simulations based on the solution of transient, spherically symmetric gas-phase equations have been reported. Major differences between the various theoretical approaches have been in the treatment of liquid-phase transport processes and the representation of high-pressure effects. These effects in general have included (i) a nonideal equation of state with appropriate mixing rules, (ii) liquid-phase solubility of ambient gases, (iii) high-pressure treatment of liquid-phase equilibrium based on the fugacity of each phase, and (iv) effect of pressure on thermo-transport properties. An extensive review of the published experimental and computational investigations is provided by Gilver and Abraham [18].

It is important to emphasize that our objective is to evaluate a high-pressure droplet vaporization model within the framework of the quasi-steady approximation, such that the model can be economically incorporated in high-pressure spray algorithms appropriate for 1–10 million node calculations for gas turbine simulations. While more advanced vaporization models based on a transient gas-phase analysis may be more desirable under high-pressure conditions, it is currently not feasible to employ them in comprehensive spray computations.

The Physical Model

An isolated multicomponent (containing N components) fuel droplet evaporating in a high-temperature high-pressure environment is analyzed. The droplet size, ambient temperature, and pressure are considered in a range that corresponds to a wide range of power requirements for a gas turbine combustor. The gas-phase processes are assumed to be quasi-steady, which implies that the characteristic gas-phase time is much shorter compared to the liquid-phase transient time as well as the time associated with the surface regression rate. This requires ([6]) that the ratio of gas density to liquid density be at least an order of magnitude smaller than unity. Other assumptions include spherical symmetry, phase-equilibrium at the droplet surface, and negligible secondary diffusion and radiation. Then, the energy and fuel-vapor species conservation equations can be written as

$$\frac{d}{dr}\left(r^2\rho v c_p(T-T_s) - r^2\rho D c_p \mathrm{Le}\frac{d(T-T_s)}{dr}\right)=0 \tag{1}$$

$$\frac{d}{dr}\left(r^2\rho v Y_i - r^2\rho D\frac{dY_i}{dr}\right)=0 \tag{2}$$

where r is the radial coordinate, v is the gas or Stefan flow velocity, Le is the gas-phase Lewis number, and Y_i is the mass fraction of ith fuel species with $i=1,2,\ldots N$. In addition, T is the ambient temperature, T_s the droplet surface temperature, ρ the gas density, c_p the gas specific heat at constant pressure, and D the diffusion coefficient, With appropriate boundary conditions, the solution of Eq. (1) at $r=r_\infty$ yields

$$\frac{\dot{m}}{4\pi\rho D\mathrm{Le}}[1/r_s-1/r_\infty]=\ln\left[1+\frac{c_p(T_\infty-T_s)}{H}\right] \tag{3}$$

while the solution of Eq. (2) at $r=r_s$ yields

$$\frac{\dot{m}}{4\pi\rho D}[1/r_s-1/r_\infty]=\ln\left[\frac{\varepsilon_i-Y_{i\infty}}{\varepsilon_i-Y_{is}}\right]. \tag{4}$$

H in Eq. (3) represents the energy supplied to the droplet (per unit mass of fuel vaporized) for heating and vaporization, and $\dot{m}$ represents the vaporization rate. Further, r_∞ is the radial location representing the ambient conditions, which are assumed to be specified at infinity for an isolated droplet, and ε_i is the fractional vaporization rate of species i, given by $\varepsilon_i=\dot{m}_i/\dot{m}$. Summing Eq. (2) over all the fuel species and integrating the resulting equation yields

$$\frac{\dot{m}}{4\pi A\rho D}[1/r_s-1/r_\infty]=\ln(1+B) \tag{5}$$

where B is the transfer number given by

$$B=\frac{Y_{fs}-Y_{f\infty}}{1-Y_{fs}}. \tag{6}$$

Equations (3), (4), and (5) can be combined to obtain expressions for ε_i and H. Details are provided in Ref. [10]. The droplet size history is computed using

$$\frac{dr_s^2}{dt}=-\frac{\dot{m}}{2\pi r_s\rho_l}. \tag{7}$$

In summary, the low pressure model for both the single and multicomponent fuel droplets considers gas-phase processes to be quasi-steady phase, equilibrium at the droplet surface, and transient liquid-phase processes represented by either the infinite-diffusion model or the diffusion-limit model ([7,9]). As discussed in the next section, the phase equilibrium is represented by the Clausius-Clapeyron relation for each fuel component, supplemented by the Raoult's law for the multicomponent case.

High-Pressure Models

Two high-pressure models are employed. The first model is based on the ideal equation of state and does not consider the solubility of gases into liquid. Consequently, the phase equilibrium at the droplet surface is represented by using the Clausius-Clapeyron relation for each fuel component, supplemented by the Raoult's law for the multicomponent case. The Clausius-Clapeyron relation can be written as

$$X_{oi} = \exp\left\{\frac{L_i M_{fi}}{R_o}\left(\frac{1}{T_{bi}} - \frac{1}{T_s}\right)\right\} \tag{8}$$

where the subscript i refers to the fuel component i, X_{oi} is the equilibrium fuel vapor mole fraction, T_{bi} the boiling temperature at a given pressure p, L_i the heat of vaporization (considered function of T_s and pressure), M_{fi} the molecular weight, and R_o the universal gas constant. The vapor mole fraction of each fuel component at the surface is calculated using the Raoult's law

$$X_{is} = X_{ils} X_{oi} \tag{9}$$

where X_{ils} is the liquid mole fraction of fuel species i at the surface. The vapor mole fraction of each fuel species at the droplet surface (Y_{is}) can be calculated from X_{ils} and M_i, while T_{bi} and L_i are calculated as

$$T_{bi} = A_1/(A_2 - \ln(P)) \tag{10}$$

$$L_i = \left(\frac{T_{ci} - T_s}{T_{ci} - T_{bni}}\right)^{0.38} L_{ni} \tag{11}$$

where $A_1 = L_{ni} \cdot M_{fi}/R_o$, $A_2 = A_1/T_{bni}$, L_{ni} is the heat of vaporization at normal boiling temperature (T_{bni}), and P is the pressure in atmosphere. The liquid-phase transient processes appear through the variables X_{ils} and T_s, and are represented by the infinite-diffusion and diffusion-limit models. These two models are described in Ref. [19]. The important difference between the low-pressure model and the first high-pressure model is that the liquid boiling temperature and heat of vaporization are considered to be pressure-dependent in the latter model.

The second high-pressure model considers the real gas behavior, the solubility of gases into the liquid, and the effect of pressure on thermo-transport properties. The real gas behavior is represented by using the Peng-Robinson equation of state ([20,21]) in the following form:

$$Z = \frac{PV}{RT} = \frac{V}{V-b} - \frac{c/RT + d - 2\sqrt{cd/RT}}{(V+b) + (b/V)(V-b)} \tag{12}$$

where Z is the compressibility factor, R the universal gas constant (82.052 atm.cm^3/mole.K), T the temperature (K), P the pressure (atm), and V the molar volume (cm^3/mole). For a pure fluid, the constants b, c, and d are given as

$$\begin{aligned} b &= 0.0778 R T_c / P_c \\ c &= a(T_c)(1+k)^2 \\ d &= a(T_c) k^2 / R T_c \\ a(T_c) &= 0.45724 R^2 T_c^2 / P_c . \end{aligned} \tag{13}$$

Here the subscript c represents critical state. Equation (12) is solved as a cubic in Z to calculate the ambient compressibility factor and density. The mixture properties (Z and ρ) at the droplet surface are obtained by employing the appropriate mixing rules ([22]). Details are provided in Ref. [23]. The vapor-liquid equilibrium at the droplet surface is expressed by the equality of chemical potential of each species in the liquid and vapor phases, and can be written as

$$x_i^V \phi_i^V = x_i^L \phi_i^L \tag{14}$$

where the fugacity coefficients ϕ_i for both the vapor and liquid phases can be written as

$$RT \cdot \ln \phi_i = \int_V^\infty [(\partial P/\partial n_i)_{T,V,n_i} - (RT/V)]dV - RT \ln Z. \tag{15}$$

Using the Peng-Robinson equation of state and the appropriate mixing rules, the fugacity coefficients can be expressed as functions of T, P, and Z. Details are provided in Ref. [23].

The latent heat of evaporation is given by

$$h_i = h_i^o - RT^2(\partial \ln \phi_i/\partial T)_{P,x_i} \tag{16}$$

where the enthalpy h_i is in J/mol, and the universal gas constant R is in J/mol/K. The vapor and liquid phases refer to the same state o. Then, the latent heat of evaporation is defined by the difference of the vapor and liquid-phase enthalpies

$$L_i = h_i^V - h_i^L \tag{17}$$

Thermophysical and Transport Properties

A detailed algorithm is developed for calculating the variable thermophysical and transport properties of both phases. For the liquid phase, the variable properties are considered for both the single-component and multicomponent fuels. For a majority of cases, the data is compiled from various sources ([20,24–28]) and is employed in the form of polynomials. All the thermo-transport properties are considered to be pressure, temperature, and species-dependent. The procedure along with the relevant equations are provided in Refs. [19] and [23].

The calculation of thermo-transport properties was confirmed by independently using the Chemkin subroutines ([16,28]) as well as by comparing with experimental data ([25–27]). As discussed in Refs. [19] and [23], the property algorithm was shown to reproduce the experimental data quite well.

The quasi-steady droplet vaporization model requires that the thermo-transport properties of the gas film in the droplet vicinity be calculated continuously as the droplet evaporates. All the gas-film mixture properties are computed at the weighted-averaged temperature and species mass fractions, obtained from the temperature and composition at the droplet surface and those at infinity, as

$$\Phi_{\text{avg}} = \alpha \Phi_{gs} + (1-\alpha)\Phi_g \tag{18}$$

where Φ is a generic quantity representing either temperature or mass fraction, and the α is selected to be as 0.7. The subscripts gs and g represent the gas-phase property at the droplet surface and outside the gas film (infinity), respectively.

The Solution Procedure

The theoretical model described above is applicable to both single-component and multicomponent fuel droplets. In the present study, the results are obtained for a bicomponent ($N=2$) and an equivalent single-component ($N=1$) fuel droplet. A general procedure involves calculating T_{bi}, L_i, and Y_{is} by using T_s at the old time-step. Then, the average gas temperature and species mass fractions are obtained from Eq. (18), and the thermo-transport properties of the gaseous mixture are calculated by using the equations described in Refs. [19] and [23]. Similarly, the liquid fuel properties, such as specific heat, thermal conductivity, and density, are computed. Note that liquid temperature used for calculating these properties is the droplet surface temperature for the infinite-diffusion model, while an average of the liquid temperatures at the droplet surface and center are used for the diffusion-limit model. The new T_s is then calculated by using the infinite-diffusion or the diffusion-limit model. Finally, the droplet radius is calculated by using Eq. (7).

Results and Discussion

First, we focus on the comparison of the vaporization characteristics of a bicomponent fuel droplet and an surrogate pure fuel droplet for conditions that correspond to the operating range of a typical gas turbine combustor. For the base case, a bicomponent fuel containing equal amounts of n-$C_{10}H_{22}$ and n-$C_{14}H_{30}$ by mass is considered, and its vaporization behavior is compared with that of pure n-$C_{12}H_{26}$ droplet. The boiling temperature of n-$C_{12}H_{26}$ is approximately equal to that of Jet-A fuel. At one atmospheric pressure, the boiling temperatures of $C_{10}H_{22}$, $C_{12}H_{26}$ and $C_{14}H_{30}$ are 447.3 K, 489.5 K, and 526.7 K. These temperatures correspond, respectively, to the initial boiling, midpoint boiling (50

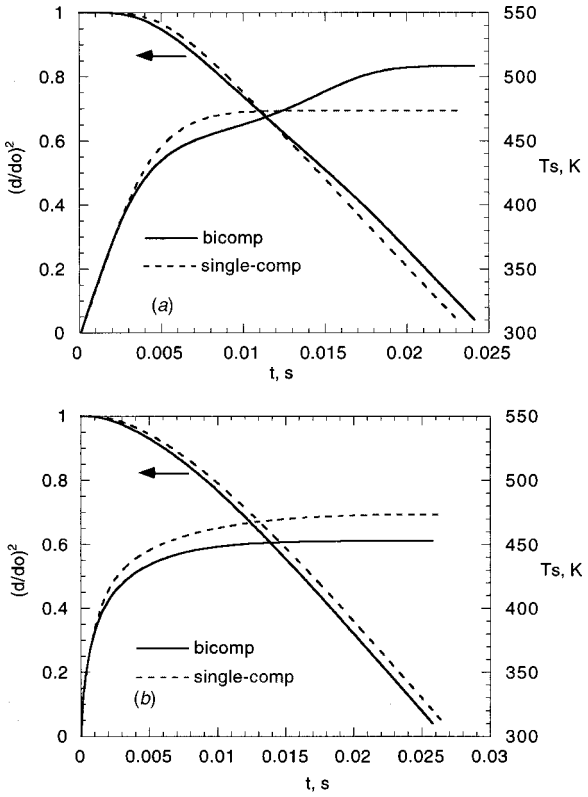

Fig. 1 Temporal histories of droplet surface area (nondimensional) and temperature for a bicomponent ($n\text{-}C_{10}H_{22}$ and $n\text{-}C_{14}H_{30}$) and an equivalent single-component ($n\text{-}C_{12}H_{26}$) fuel droplet. Predictions of infinite-diffusion and diffusion-limit models are shown in Figs. 1(*a*) and 1(*b*), respectively. Ambient temperature=1500 K, pressure=1 atm, and initial droplet diameter and temperature are 100 μm and 300 K, respectively.

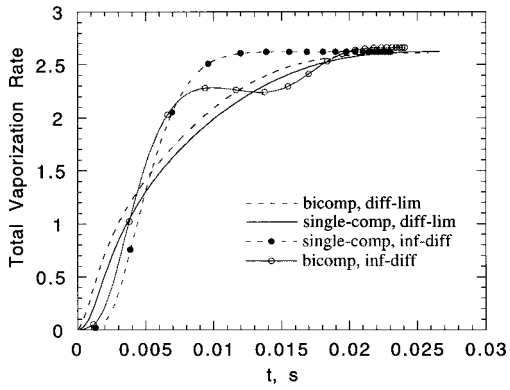

Fig. 2 Comparison of total vaporization rates (nondimensional) for a bicomponent and an equivalent single-component fuel droplet predicted using the infinite-diffusion and diffusion-limit models for the conditions of Fig. 1

percent) and final boiling for Jet-A fuel. The calculations presented for the base case are for a droplet with initial diameter of 100 μm, which is placed in an ambient with temperature and pressure of 1500 K and one atmosphere respectively. The 1500 K represents a typical incipient lean blowout temperature for ground-idle operation. Consequently, these calculations are representative for estimating the effect of heatup and vaporization models on lean blowout fuel-air ratios.

Figure 1 presents the vaporization and surface temperature histories of a bicomponent ($n\text{-}C_{10}H_{22}$ and $n\text{-}C_{14}H_{30}$) and an equivalent single-component ($n\text{-}C_{12}H_{26}$) droplets. The predictions of infinite-diffusion and diffusion-limit modes are shown in Figs. 1(*a*) and 1(*b*), respectively. The overall differences in the vaporization histories of bicomponent and single-component droplets are small, indicating that a suitably selected single-component fuel can be used to represent the vaporization behavior of a bicomponent fuel. There are, however, differences in the temporal variation of surface temperature (T_s) for the bicomponent and single-component fuels. For the bicomponent case, the infinite-diffusion model predicts a batch-distillation type behavior, see Fig. 1(*a*). Initially, the bicomponent droplet has lower surface temperature compared to the single-component droplet, as T_s is limited by the boiling temperature of volatile component, but higher vaporization rate since the surface vapor concentration of volatile component is higher (even though the surface temperature is lower) than that for the single-component fuel. However, later in the lifetime, the bicomponent droplet has higher T_s, which is now governed by the boiling temperature of less volatile component, but a lower vaporization rate due to the presence of less volatile fuel at the surface. For the diffusion-limit model, the bicomponent droplet has lower surface temperature but higher vaporization rate compared to the single-component droplet throughout its lifetime. This is due to the presence of more volatile component at the bicomponent droplet surface.

The comparison of the total vaporization rates of bicomponent and single-component fuels predicted using the infinite-diffusion and diffusion-limit models is shown in Fig. 2. The total vaporization rate is a better indicator of how well a single-component fuel can represent the vaporization behavior of a bicomponent fuel spray. Results indicate that by using the diffusion-limit model, the vaporization rate of a bicomponent fuel droplet can be well represented by an equivalent single-component droplet. In contrast, the use of infinite-diffusion model leads to more discrepancies between the vaporization rates of bicomponent and single-component fuel droplets. This is attributable to the batch-distillation behavior predicted by the infinite-diffusion model for the bicomponent droplet. The batch-distillation behavior is characterized by the vaporization of the more volatile component, followed by leveling of the vaporization rate since the less volatile component is being heated during this time, and subsequent resumption of the higher vaporization rate due to the vaporization of less volatile component.

In order to examine whether this behavior is observed for a wide range of conditions in a gas turbine combustor, results were obtained for different ambient temperature (800 K) and initial droplet diameter (25 μm). These conditions are relevant to premixing, prevaporizing systems at high-power conditions, especially for dry low-emission combustors. For these cases, using the diffusion-limit model, the total vaporization rate of a bicomponent fuel droplet was observed to be well represented by that of an equivalent single-component droplet.

Multicomponent Effects During Initial Starting and Ignition

As known from experience and confirmed by simple simulations here, spray-droplet heatup and evaporation rates during start (ignition and flame propagation) are impacted significantly by the fuel properties. Model results for heatup and evaporation are presented for a gas temperature of 373 K. Figure 3 shows the temporal variation of the droplet diameter squared and surface temperature for the bicomponent and single-component cases. Contrary to the high-gas-temperature cases discussed above, there are now significant differences in the vaporization histories of bicomponent and the corresponding single-component fuel droplets.

Figure 4 presents the comparison of the total vaporization rates for the bicomponent and single-component fuel droplets predicted using the two models. It is evident that for these conditions, the

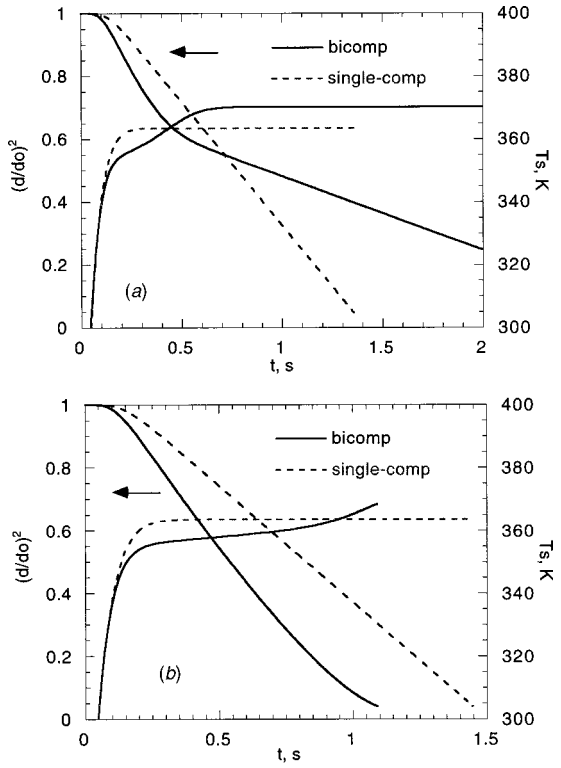

Fig. 3 Temporal histories of droplet surface area (nondimensional) and temperature for a bicomponent ($n\text{-}C_{10}H_{22}$ and $n\text{-}C_{14}H_{30}$) and an equivalent single-component ($n\text{-}C_{12}H_{26}$) fuel droplet. Predictions of infinite-diffusion and diffusion-limit models are shown in Figs. 3(*a*) and 3(*b*), respectively. Ambient temperature=373 K, pressure=1 atm, and initial droplet temperature=233 K.

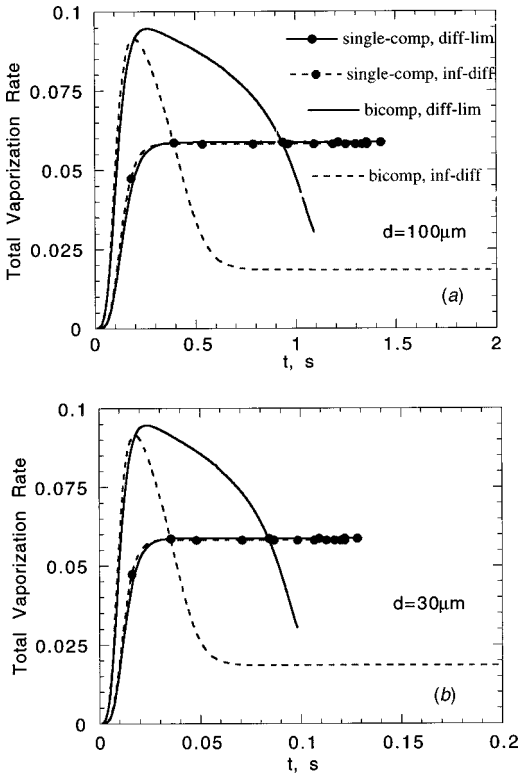

Fig. 4 Total vaporization rates (nondimensional) for a bicomponent and an equivalent single-component fuel droplet predicted using the infinite-diffusion and diffusion-limit models. Initial droplet diameter is 100 μm for Fig. 4(*a*) and 30 μm for Fig. 4(*b*). Other conditions are the same as those in Fig. 3.

vaporization behavior of a bicomponent droplet cannot be simulated by an equivalent pure fuel droplet, as both the instantaneous vaporization rate and the droplet life time differ considerably for the bicomponent and single-component cases. This can be attributed to the fact that the ambient temperature for this case is much lower than the boiling temperature of the less volatile component. In addition, it is indicated that while the differences in the predictions of the two models for the bicomponent case are quite significant, they are negligible for the corresponding single-component case. A similar behavior is observed when the initial droplet diameter is reduced to 30 microns, except that the life time of the 30-micron droplet is reduced by a factor of about 10 compared to that of the 100-micron droplet. An important implication of this result is that the ignition characteristics of a multicomponent fuel spray cannot be simulated by using a single-component fuel spray model, since the ignition behavior for the former is governed by the presence of the volatile component ([29]).

Effect of Pressure

Figure 5 presents a comparison of the vaporization characteristics of bicomponent and equivalent single-component fuel droplets at different pressures. The corresponding plots showing the temporal variation of surface temperature are given in Fig. 6. The results in Figs. 5 and 6 are obtained using the first high-pressure vaporization model. Important observations from these figures are as follows.

1 For both the bicomponent and single-component fuel droplets, the droplet lifetime is not altered significantly as the ambient pressure is increased. However, the droplet heatup time becomes a more significant part of droplet lifetime, increasing from about 20 to 40 percent of the lifetime as p is increased from 1 to 15 atm. The increase in droplet heatup time is caused by the increase in the fuel boiling temperature with pressure. The boiling temperature of n-dodecane increases from 489.5 K to 654.9 K as pressure is increased from $p=1$ atm to 15 atm. Correspondingly, for the bicomponent case, the boiling temperature of $n\text{-}C_{10}H_{22}$ (volatile component) increases from 447.3 K to 601.6 K, while that of $n\text{-}C_{14}H_{30}$ increased from 526.7 K to 701.3 K. Obviously, this would increase the droplet heatup time for a fixed ambient temperature for both the bicomponent and single-component cases. Note that an increase in p decreases the latent heat of evaporation, which would increase the vaporization rate. However, this effect is largely compensated by an increase in the droplet heatup time. Note that for the convective case, another effect of pressure appears through its influence on the droplet Reynolds number which increases as the pressure is increased. This would enhance the vaporization rate.

2 The difference between the predictions of infinite-diffusion and diffusion-limit models is small at low pressures, but becomes increasingly more noticeable at higher pressures. As pressure increases, the infinite-diffusion model predicts increasingly higher vaporization rate compared to that by the diffusion-limit model. For example, at $p=15$ atm, the droplet lifetime predicted by this model is about 40 percent shorter. This can be attributed to two effects. First, it overpredicts the droplet surface temperature (during most of its lifetime) compared to that by the diffusion-limit model. Second, the heat of evaporation is reduced at higher pressures, so that even small differences in surface temperature can cause significant changes in the transfer number B.

3 For the bicomponent case, the batch distillation process, predicted by the infinite-diffusion model at $p=1$ atm, becomes less noticeable at higher pressures. This can be attributed to a decrease in relative volatility differential at higher pressures. Note that

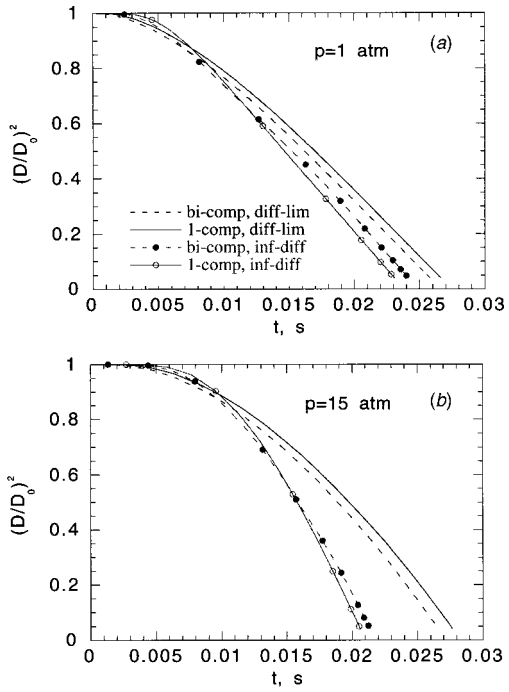

Fig. 5 Temporal variation of droplet surface area (nondimensional) for a bicomponent ($n\text{-}C_{10}H_{22}$ and $n\text{-}C_{14}H_{30}$) and an equivalent single-component ($n\text{-}C_{12}H_{26}$) fuel droplet for pressure of 1 atm (Fig. 5(*a*)) and 15 atm (Fig. 5(*b*)). Predictions of the infinite-diffusion and diffusion-limit models are shown. The gas temperature is 1500 K, and initial droplet diameter is 100 μm.

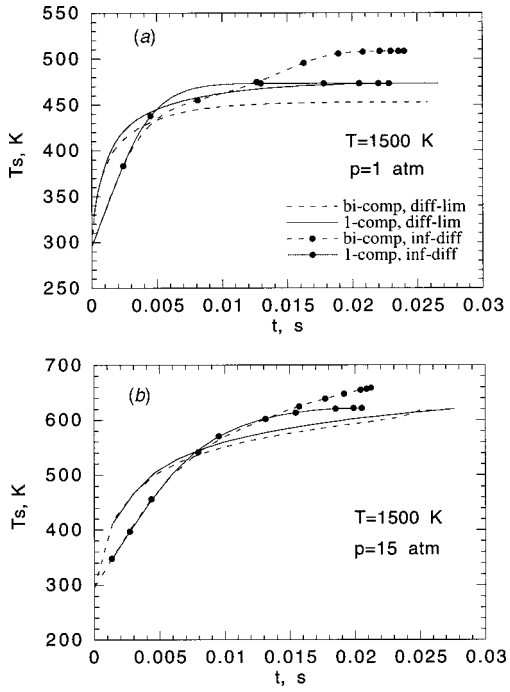

Fig. 6 Temporal variation of droplet surface temperature for a bicomponent and an equivalent single-component fuel droplet for the conditions of Fig. 5

batch distillation process at $p=1$ atm is easily discernible in the temperature plot for the infinite-diffusion model in Fig. 6(*a*).

4 The comparison of the temporal variations of droplet diameter squared and surface temperature for the bicomponent and single-component cases indicates that for high ambient temperatures, a single-component droplet model can simulate the vaporization behavior of a bicomponent fuel droplet reasonably well over a wide range of pressures. In fact, the predicted vaporization behavior is significantly more sensitive to the droplet heating model used rather than to the liquid fuel composition. In addition, the representation of a bicomponent fuel droplet by an equivalent single-component seems to become increasingly better as the pressure is increased. This is apparently due to the increased droplet heatup time and the reduced volatility differential at higher pressures.

Validation of the High-Pressure Vaporization Model

The second quasi-steady high-pressure model was validated by comparing its predictions with the available experimental data. Figure 7 presents the predicted liquid-vapor equilibrium for nitrogen/n-heptane mixtures in terms of the equilibrium nitrogen mole fraction as a function of pressure and temperature. The predicted vapor and liquid mole fractions of N_2 show excellent agreement with the experimental data of Knapp et al. [24].

The vaporization history predictions are validated using the experimental data of Stengele et al. [12]. In the experiential study, freely falling n-heptane droplets in a stagnant, high-pressure, high-temperature nitrogen environment were considered. The droplet diameter and velocity were measured along the droplet trajectory using a high-speed video and stroboscope lamp. Since the measured data were provided along the droplet trajectory, the following equations are employed in the computational model to calculate the temporal variation of droplet position and velocity:

$$\frac{dx_d}{dt} = u_d \tag{19}$$

$$\frac{du_d}{dt} = \frac{3\rho C_d}{4\rho_l d_d}|u-u_d|(u-u_d) + (1-\rho/\rho_l)g \tag{20}$$

and the drag coefficient is calculated using the same correlation as used in the cited study ([12])

$$C_d = [0.36 + 5.48\,\mathrm{Re}_d^{-0.573} + 24/\mathrm{Re}_d](1+B)^{-0.2} \tag{21}$$

$$\mathrm{Re}_d = \rho|u-u_d|d_d/\mu. \tag{22}$$

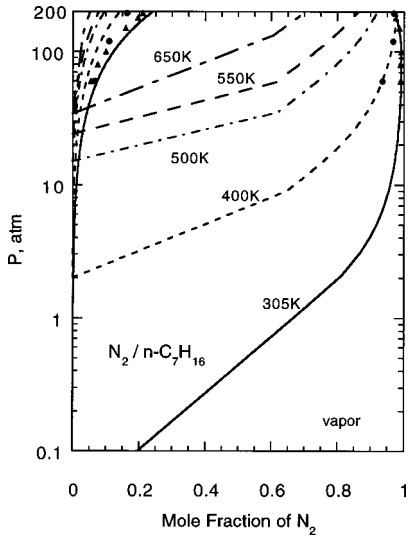

Fig. 7 Pressure-mole fraction diagram for nitrogen/n-heptane mixtures, calculated using the Peng-Robinson equation of state. Experimental data from Ref. [24] at 305 K and 400 K are also shown.

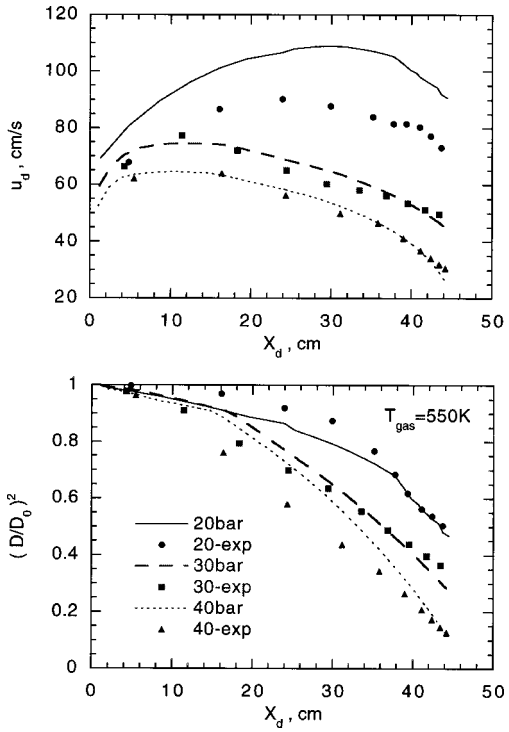

Fig. 8 Comparison of the predicted and measured (n-heptane) droplet velocity and nondimensional surface area along the trajectory for three different ambient pressures. Ambient temperature is 550 K and initial droplet diameter is 780 μm.

The gas velocity (u) in the above equations was taken to be zero in the experimental study. The gas density (ρ) and viscosity (μ) are assumed to be ambient density and gas film viscosity, respectively.

Figure 8 presents the comparison of the predicted and measured droplet velocity and surface area for three different ambient pressures. In general, predictions of the second high-pressure model are in reasonably good agreement with experimental data over a wide range of pressures. As p is increased, the computed and measured droplet velocity decrease, which can be attributed to the increased gas density at higher pressures. As indicated in Eq. (20), the increased gas density diminishes the gravitational force, but enhances the viscous drag force. Note the droplet Reynolds number increases as p is increased, but C_d is nearly independent of Re_d in the high Re_d limit. For $p=20$ atm, differences in the predicted and measured surface area are attributable to the underprediction of the droplet velocity, with the implication that an accurate calculation of droplet velocity and trajectory is critical for an accurate prediction of droplet vaporization history. At $p=40$ atm, the numerical model underpredicts the vaporization rate compared to the experimental data. This is indicative of the limit of the quasi-steady vaporization model at high pressures.

Conclusions

In this paper, we have examined the multicomponent and high-pressure effects on the vaporization behavior of gas turbine fuels. The state-of-the-art vaporization models along with a detailed algorithm for the computation of liquid and gas-phase thermo-transport have been employed to examine whether the vaporization behavior of a multicomponent fuel droplet can be simulated by a surrogate pure fuel droplet. The vaporization history and other relevant properties of a bicomponent fuel droplet have been compared with those of an equivalent single-component droplet under a wide range of conditions that exist in a typical gas turbine combustor. In particular, three typical operating conditions have been considered: (1) lean blowout for ground-idle operation; (2) premixing, prevaporizing system at high-power conditions; and (3) startup (ignition and flame propagation) conditions. In addition, two high-pressure vaporization models within the quasi-steady framework have been investigated. The first model considers the effect of pressure on thermodynamic and transport properties, while the second model also considers the nonideal gas effects and dissolution of gases into the liquid. Important observations are as follows:

1 Under high-power conditions, the vaporization behavior of a gas turbine fuel is well represented by an equivalent single-component (50 percent boiling point) fuel. However, the comparison of the total vaporization rates of bicomponent and single-component fuels indicates significant differences in the predictions of the infinite-diffusion and diffusion-limit models. Using the diffusion-limit model, the vaporization rate of a bicomponent fuel droplet can be well represented by an equivalent single-component droplet for a wide range of conditions. In contrast, the use of the infinite-diffusion model indicates discrepancies between the vaporization rates of bicomponent and single-component fuel droplet. Since the total vaporization rate is a better indicator of how well a single-component fuel can represent the vaporization behavior of a multicomponent spray, it is recommended that a diffusion-limit model or a effective-diffusivity model be employed in the spray models. This conclusion also applies to the prediction of vaporization rates of gas turbine fuels for premixing, prevaporizing systems at high-power conditions.

2 Liquid and gas-phase properties change considerably during the droplet lifetime. Consequently, an accurate calculation of the thermo-transport properties should be an essential part of spray computations.

3 The droplet lifetime is relatively insensitive to pressure. However, the droplet heatup time becomes a more significant part of droplet lifetime at higher pressures. Consequently, differences between the predictions of the infinite-diffusion and diffusion-limit models become increasingly more noticeable at elevated pressures. The infinite-diffusion model predicts significantly higher vaporization rate compared to the diffusion-limit model for both single-component and bicomponent fuel droplets. For example, at $p=15$ atm, this model predicts 40 percent shorter droplet lifetime compared to the diffusion-limit model.

4 The representation of a bicomponent fuel droplet by an equivalent single-component becomes increasingly better at higher pressures. In fact, the predicted vaporization behavior is significantly more sensitive to the droplet heating model rather than to the liquid fuel composition. This can be attributed to a significant increase in droplet heatup time, and a reduction in the relative volatility differential between the constituent fuels at high pressure.

5 For ignition, LBO, and idle operation, the multicomponent fuel effects become relatively important, i.e., using a single-component droplet to represent multicomponent effects lead to unacceptable results, especially when the infinite-diffusion model is employed.

6 The predicted vaporization histories of n-heptane droplets using a quasi-steady high-pressure model show good agreement with the measured data over a wide range of pressures. The high-pressure model incorporates the nonideal gas behavior, dissolution of gases into the liquid, and dependence of thermo-transport properties on pressure. At $p=40$ atm, which is above the critical pressure of the fuel, the model underpredicts the vaporization rate compared to the experimental data, which is perhaps indicative of the high-pressure limit of our quasi-steady vaporization model.

Acknowledgment

This work has been funded by the GE Aircraft Engines.

References

[1] Westbrook, C. K., Pitz, W., and Warnatz, J., 1988, ''A Detailed Chemical Kinetic Reaction Mechanism for the Oxidation of Iso-Octane and n-Heptane over an Extended Temperature Range,'' Proc. Combust. Inst., **22**, pp. 893–902.

[2] Callahan, C. V., Held, T. J., Dryer, F. L., Minetti, R., Ribaucour, M., Sochet, L. R., Faravelli, T., Gaffuri, P., and Ranzi, E., 1996, ''Experimental Data and Kinetic Modeling of Primary Reference Fuel Mixtures,'' Proc. Combust. Inst., **26**, pp. 739–746.

[3] Newbold, F. R., and Amundson, N. R., 1973, ''A Model for Evaporation of a Multicomponent Droplet,'' AIChE J., **19**, pp. 22–30.

[4] Landis R. B., and Mills, A. F., 1974, ''Effects of Internal Resistance on the Vaporization of Binary Droplets,'' Fifth International Heat Transfer Conference, Paper B7-9, Tokyo, Japan.

[5] Law, C. K., 1982, ''Recent Advances in Droplet Vaporization and Combustion,'' Prog. Energy Combust. Sci., **8**, pp. 169–195.

[6] Tong, A. Y., and Sirignano, W. A., 1986, ''Multicomponent Droplet Vaporization in a High Temperature Gas,'' Combust. Flame, **66**, pp. 221–235.

[7] Abramzon, B., and Sirignano, W. A., 1989, ''Droplet Vaporization Models for Spray Combustion Calculations,'' **32**, No. 9, pp. 1605–1618.

[8] Chen, G., Aggarwal, S. K., Jackson, T. A., and Switzer, G. L., 1997, ''Experimental Study of Pure and Multicomponent Fuel Evaporation in a Heated Air Flow,'' Atomization Sprays, **7**, pp. 317–337.

[9] Aggarwal, S. K., 1987, ''Modeling of Multicomponent Fuel Spray Vaporization,'' Int. J. Heat Mass Transf., **30**, No. 9, pp. 1949–1961.

[10] Canada, G. S., and Faeth, G. M., 1974, ''Fuel Droplet Burning Rates at High Pressures,'' Proc. Combust. Inst., **14**, pp. 1345–1354.

[11] Nomura, H., Ujiie, Y., Rath, H. J., Sato, J., and Kono, M., 1996, ''Experimental Study on High-Pressure Droplet Evaporation Using Microgravity Conditions,'' Proc. Combust. Inst., **26**, pp. 1267–1273.

[12] Stengele, J., Willmann, M., and Wittig, S., 1997, ''Experimental and Theoretical Study of Droplet Vaporization in High Pressure Environment,'' ASME Paper 97-GT-151.

[13] Hsieh, K. C., Shuen, J. S., and Yang, V., 1991, ''Droplet Vaporization in High Pressure Environments: Near Critical Conditions,'' Combust. Sci. Technol., **76**, pp. 111–132.

[14] Curtis, E. W., and Farrel, P. W., 1992, ''A Numerical Study of High-Pressure Droplet Vaporization,'' Combust. Flame, **90**, pp. 85–102.

[15] Jia, J. D., and Gogos, G., 1993, ''High-Pressure Droplet Vaporization: Effects of Liquid-Phase Gas Solubility,'' Int. J. Heat Mass Transf., **36**, pp. 2403–2415.

[16] Stengele, J., Bauer, H.-J., and Wittig, S., 1996, ''Numerical Study of Bicomponent Droplet Vaporization in a High Pressure Environment,'' ASME Paper 96-GT-442.

[17] Zhu, G., and Aggarwal, S. K., 2000, ''Transient Supercritical Droplet Evaporation With Emphasis on the Effects of Equation of State,'' Int. J. Heat Mass Transf., **43**, No. 7, pp. 1157–1171.

[18] Gilver, S. D., and Abraham, J., 1996, ''Supercritical Droplet Vaporization and Combustion Studies,'' Prog. Energy Combust. Sci., **22**, pp. 1–28.

[19] Aggarwal, S. K., Shu, Z., Mongia, H., and Hura, H., 1998, ''Multicomponent Fuel Effects on the Vaporization of a Surrogate Single-Component Fuel Droplet,'' Paper 98-0157, 36th Aerospace Sciences Meeting, Reno, NV, Jan. 12–15.

[20] Reid, R. C., Prausnitz, J. M., and Polin, B. E., 1987, *The Properties of Gases and Liquids*, 4th Ed., McGraw-Hill, New York.

[21] Ruszalo, R., and Hallett, W. L. H., 1992, ''A Model for the Autoignition of Single Liquid Droplets at High Pressure,'' Combust. Sci. Technol., **86**, pp. 183–197.

[22] Benmekki, E. H., 1988, ''Fluid Phase Equilibria with Theoretical and Semi-Empirical Equation of State Model,'' Ph.D. thesis, University of Illinois at Chicago, Chicago, IL.

[23] Aggarwal, S. K., Shu, Z., Mongia, H., and Hura, H. S., 1998, ''Multicomponent and Single-Component Fuel Droplet Vaporization Under High Pressure Conditions,'' Paper 98-3933, 34th AIAA/ASME/SAE/ASEE Joint Propulsion Conference, Cleveland, OH, July 13–15.

[24] Knapp, H., Doring, R., Oellrich, L., Plocker, U., and Prausnitz, J. M., 1982, ''Vapor-Liquid Equilibria for Mixtures of Low Boiling Substances,'' J. Chem. Eng. Data **VI** DECHEMA Frankfurt.

[25] Vargaftik, N. B., and Touloukian, Y. S., 1983, *Handbook of Physical Properties of Liquids and Gases: Pure Substances and Mixture*, 2nd Ed., Hemisphere, Washington, DC.

[26] Lide, R. David, 1994, *CRC Handbook of Chemistry and Physics 1913–1995*, 74th Ed., Chemical Rubber Publishing Company, Boca Raton, FL.

[27] Ho, C. Y., Liley, P. C., Makita, T., and Tanaka, Y, 1988, CINDAS, *Data Series on Material Properties Volume V-1: Properties of Inorganic and Organic Fluids*, Hemisphere, Washington, DC.

[28] Kee, R. J., Miller, J. A., and Warnatz, J., 1983, ''A Fortran Program Package for the Evaluation of Gas-Phase Viscosities, Conductivities, and Diffusion Coefficients,'' Sandia National Laboratories Report SAND83-8209.

[29] Aggarwal, S. K., 1989, ''Ignition Behavior of a Dilute Multicomponent Fuel Spray,'' Combust. Flame, **76**, pp. 5–15.